The LINNEAN SOCIETY of London BIOLOGICAL Journal of the Linnean Society

Biological Journal of the Linnean Society, 2013, **110**, 346–361. With 6 figures

Multiple cases of asymmetric introgression among horseshoe bats detected by phylogenetic conflicts across loci

XIUGUANG MAO[1,2], VU D. THONG[3], PAUL J. J. BATES[4], GARETH JONES[5], SHUYI ZHANG[1] and STEPHEN J. ROSSITER[2]*

[1]*Institute of Molecular Ecology and Evolution, Institute for Advanced Studies in Multidisciplinary Science and Technology, East China Normal University, Shanghai 200062, China*
[2]*School of Biological and Chemical Sciences, Queen Mary University of London, London E1 4NS, UK*
[3]*Institute of Ecology and Biological Resources, 18 Hoang Quoc Viet Road, Cau Giay District, Hanoi, Vietnam*
[4]*Harrison Institute, Centre for Systematics and Biodiversity Research, Bowerwood House, St Botolph's Road, Sevenoaks, Kent TN13 3AQ, UK*
[5]*School of Biological Sciences, University of Bristol, Woodland Road, Bristol BS8 1UG, UK*

Received 18 March 2013; revised 6 May 2013; accepted for publication 6 May 2013

Phylogenetic discordance among taxa can provide powerful insights into past episodes of introgressive hybridization, as well as lineage sorting. Previously, we showed that the taxonomically distinct taxon *Rhinolophus sinicus septentrionalis* has undergone historical introgression with its sympatric sister subspecies *Rhinolophus sinicus sinicus*. To examine in more detail the extent of gene flow between these two taxa, and also between these and their sister species *Rhinolophus thomasi*, we obtained new samples from China, Myanmar, and Vietnam, and combined new and published genetic data from these, *Rhinolophus rouxii*, and *Rhinolophus indorouxii* from India. Phylogenetic analyses revealed three separate cases of discordance: between *R. s. septentrionalis* and adjacent populations of *R. s. sinicus*, between *R. s. septentrionalis* and *R. thomasi* and between eastern populations of *R. s. sinicus* and a newly-identified lineage. In both former cases, the mitochondrial DNA introgression appears to be asymmetric, which is likely to have resulted from mating between *R. s. septentrionalis* females with smaller *R. s. sinicus* and *R. thomasi* males, although we cannot rule out other scenarios completely. Further conflicts between genetic data and accepted species arrangements across the genus, with paraphyly of members of the *rouxii*-group, suggest the need for a thorough systematic revision of relationships within this group. *Biological Journal of the Linnean Society*, 2013, **110**, 346–361.

ADDITIONAL KEYWORDS: discordance – gene flow – reproductive isolation.

INTRODUCTION

Delimiting taxonomic boundaries is fundamental to an understanding of the evolutionary origin of new species, and is a prerequisite for effective conservation management. Inferences based on morphological characters alone are frequently confounded by the strong effects of selection for phenotypic variations (Avise, 1994). Therefore, approaches that combine molecular markers and morphological data are becoming increasingly popular. Yet, although many such early studies relied on maternally-inherited mitochondrial (mt)DNA markers alone (Avise, 2000), these reflect only a limited fraction of the evolutionary history of a lineage (Avise, 1994; Zhang & Hewitt, 2003; Ballard & Whitlock, 2004) and there is now a growing trend for studies of taxonomy, phylogeography, and population

*Corresponding author. E-mail: s.j.rossiter@qmul.ac.uk

genetics to sample information from both mtDNA and nuclear (nc)DNA loci (Zhang & Hewitt, 2003).

An emerging outcome of multilocus studies is the frequency with which different gene genealogies differ in relation to one other, as well as with known taxonomic relationships (Maroja, Andres & Harrison, 2009; Singhal & Moritz, 2012). Several scenarios have been proposed to explain these conflicts, including incomplete lineage sorting of ancestral polymorphisms (Edwards & Beerli, 2000; Barrowclough & Zink, 2009), introgressive hybridization (Funk & Omland, 2003), genetic incompatibilities between genomes (Rand, Haney & Fry, 2004), and sex-biased dispersal (Turmelle, Kunz & Sorenson, 2011). Of these, introgressive hybridization is of particular interest to evolutionary biologists (Arnold, 1997; Barton, 2001) because of its potential roles in speciation (Mavárez *et al*., 2006; Larsen, Marchán-Rivadeneira & Baker, 2010) and adaptive radiation (Mallet *et al*., 2007; Grant & Grant, 2008).

MtDNA introgression appears to occur more frequently than nuclear introgression (Bachtrog *et al*., 2006; Klymus *et al*., 2010), in part because mitochondrial genes have a cytoplasmic origin and most are not associated with those nuclear loci that impact on hybrid fitness (Coyne & Orr, 2004). Moreover, mtDNA introgression is usually asymmetric from a particular donor taxon to a recipient taxon (Gomes *et al*., 2009; Mao *et al*., 2010a, b). Explanations for asymmetric introgression include the mechanical barrier model in which a mismatch between the genitalia of different species prevents certain combinations of mating (Coyne & Orr, 2004), a range expansion model in which neutral genes typically flow and spread from the local species to the invading species (Currat *et al*., 2008; Excoffier, Foll & Petit, 2009), adaptive introgression in which selection favors the movement of advantageous genes in one direction (Morgan *et al*., 2010), and, finally, the movement of the hybrid zone (Buggs, 2007).

Closely-related taxa with overlapping ranges that have not yet undergone complete reproductive isolation provide ideal systems to study patterns of introgressive hybridization. Horseshoe bats (family Rhinolophidae) have undergone a rapid evolutionary diversification and several species and/or subspecies occur in sympatry with each other. We previously investigated the origin of the geographically limited and distinct taxon *Rhinolophus sinicus septentrionalis* and found evidence of past mtDNA introgression with this taxon's more widespread and sympatric sister subspecies, *Rhinolophus sinicus sinicus* (Mao *et al*., 2013b). Within the horseshoe bats, these two taxa are currently recognized as belonging to the *rouxii*-group, along with *Rhinolophus thomasi* that occurs sympatrically with *R. sinicus* and is considered to be its sister species, as well as two other related species further west: *Rhinolophus rouxii* and the recently proposed new taxon *Rhinolophus indorouxii* (Chattopadhyay *et al*., 2012). All of these five taxa are superficially difficult to separate from each other based on morphology alone and, as a result, have been subject to previous taxonomic revisions (Thomas, 2000; Csorba, Ujhelyi & Thomas, 2003). Given that mtDNA introgression has already been documented between *R. s. sinicus* and *R. s. septentrionalis*, as well as among some other horseshoe bat taxa (Mao *et al*., 2010a, b, 2013a), the present study aimed to determine the extent to which mtDNA introgression has occurred more widely among members of the *rouxii*-group. In particular, we were interested in assessing whether introgression could account for morphological confusion in this group (Csorba *et al*., 2003; Chattopadhyay *et al*., 2012). Accordingly, we collected new samples of *R. thomasi* and *R. sinicus*, and screened these at one mitochondrial gene, two nuclear genes, and eight microsatellite loci for comparisons with existing datasets from *R. s. sinicus* and *R. s. septentrionalis.* In addition, we obtained, analyzed, and compared our mitochondrial data with the published data available for *R. rouxii* and *R. indorouxii*.

MATERIAL AND METHODS

Ethics statement

In China, bats were sampled nonlethally by taking wing membrane biopsies and all animals were immediately released *in situ.* Ethics clearance was approved by the National Animal Research Authority, East China Normal University (approval ID 20080209). All bats from Myanmar or Vietnam were collected as vouchers under research permits awarded to the Harrison Institute (HZM: formerly Harrison Zoological Museum) or the Institute of Ecology and Biological Resources (IEBR).

Bat measurement, sample collection, and DNA extraction

We sampled nine individuals initially identified as *R. thomasi* from western China and two from central Myanmar (i.e. museum specimen codes from HZM are SH7 and SH14), and 14 initially identified as *R. s. sinicus* from northern Vietnam (i.e. museum specimen codes from IEBR are T.221109.1, T.221109.4-8, T.221109.10-11 and T.110708.12). For each bat, we measured the forearm with dial calipers, and the body mass with a Pesola spring balance. By measuring the forearm of the bats, we aimed to assess whether differences in body size could explain any

Table 1. Summary of sample size for molecular analysis in each locality

Taxon	Number	Locality	*Cytb*	*Chd1*	*SWS1*	Microsatellite
Rhinolophus sinicus sinicus (East)	1	Qingyang, Anhui, China	1	1	1	1
Rhinolophus sinicus sinicus (East)	2	Jingxian, Anhui, China	6	1	2	6
Rhinolophus sinicus sinicus (East)	3	Huashanmiku, Anhui, China	7	4	2	11
Rhinolophus sinicus sinicus (East)	4	Sanling mountain, Jiangxi, China	8	6	2	12
Rhinolophus sinicus sinicus (East)	5	Qingfeng cave, Jiangxi, China	5	1	1	5
Rhinolophus sinicus sinicus (East)	6	Qinhui cave, Jiangxi, China	5	2	–	6
Rhinolophus sinicus sinicus (East)	7	Longhu mountain, Jiangxi, China	5	2	2	6
Rhinolophus sinicus sinicus (East)	8	Lijia country, Jiangxi, China	8	5	3	13
Rhinolophus sinicus sinicus (East)	9	Wuyishan baohuqu, Fujian, China	10	9	5	26
Rhinolophus sinicus sinicus (East)	10	Wuyishan tiliqiao, Fujian, China	1	1	1	2
Rhinolophus sinicus sinicus (East)	11	Wuyishan Yanzijiao, Fujian, China	1	1	1	2
Rhinolophus sinicus sinicus (East)	12	Taihe, Jiangxi, China	8	3	2	16
Rhinolophus sinicus sinicus (East)	13	Jinggang mountain, Jiangxi, China	2	2	–	2
Rhinolophus sinicus sinicus (East)	14	Xingguo, Jiangxi, China	3	3	1	5
Rhinolophus sinicus sinicus (East)	15	Taining, Fujian, China	4	5	4	11
Rhinolophus sinicus sinicus (East)	16	Jiangle, Fujian, China	4	2	1	4
Rhinolophus sinicus sinicus (East)	17	Mingxi, Fujian, China	2	–	–	2
Rhinolophus sinicus sinicus (East)	18	Yongan, Fujian, China	1	1	–	2
Rhinolophus sinicus sinicus (East)	19	Liancheng, Fujian, China	4	3	2	4
Rhinolophus sinicus sinicus (East)	20	Shanghang, Fujian, China	2	2	1	4
Rhinolophus sinicus sinicus (East)	21	Guilin, Guangxi, China	8	2	3	10
Rhinolophus sinicus sinicus (East)	22	Ruyuan, Guangdong, China	1	–	1	1
Rhinolophus sinicus sinicus (East)	23	Luofushan, Guangdong, China	5	6	3	6
Rhinolophus sinicus sinicus (Central)	24	Zhangjiajie, Hunan, China	7	1	2	10
Rhinolophus sinicus sinicus (Central)	25	Yongshun, Hunan, China	1	–	–	4
Rhinolophus sinicus sinicus (Central)	26	Jishou, Hunan, China	10	2	1	12
Rhinolophus sinicus sinicus (Central)	27	Fenghuang, Hunan, China	1	–	–	2
Rhinolophus sinicus sinicus (Central)	28	Wuchuan, Guizhou, China	2	1	1	1
Rhinolophus sinicus sinicus (Central)	29	Anlong, Guizhou, China	2	1	1	1
Rhinolophus sinicus sinicus (Central)	30	Emeishan, Sichuan, China	3	3	2	3
Rhinolophus sinicus sinicus (HND)	35	Yinggeling, Hainan, China	7	9	9	19
Rhinolophus sinicus sinicus (HND)	36	Wuzhishan, Hainan, China	2	3	3	3
Rhinolophus sinicus sinicus (HND)	37	Qiongzhong, Hainan, China	–	3	3	13
Rhinolophus sinicus sinicus (HND)	38	Baoqing, Hainan, China	1	1	1	3
Rhinolophus sinicus sinicus (HND)	39	Lingshui, Hainan, China	3	1	1	5
Rhinolophus sinicus sinicus (HND)	40	Jianfengling, Hainan, China	1	1	–	1
Rhinolophus sinicus sinicus (HND)	41	Maogan, Hainan, China	3	–	–	3
Rhinolophus sinicus septentrionalis	31	Huize, Yunnan, China	7	1	1	11
Rhinolophus sinicus septentrionalis	32	Jiuxiang, Yunnan, China	1	1	–	1
Rhinolophus sinicus septentrionalis	33	Fumin, Yunnan, China	3	–	–	3
Rhinolophus sinicus septentrionalis	34	Yongde, Yunnan, China	10	5	3	11
Rhinolophus thomasi	44	Longling, Yunnan, China	8	6	3	8
Rhinolophus thomasi	45	Jinuo, Yunnan, China	1	1	1	1
Rhinolophus thomasi	46	Shan State, Myanmar	2	–	–	–
Rhinolophus sinicus ssp	42	Co Ma NR, Vietnam	4	4	2	4
Rhinolophus sinicus ssp	43	Muong Do NR, Lan Cave, Vietnam	1	1	1	1
Rhinolophus sinicus ssp	47	Xuan Son, Ninh Binh,Vietnam	8	–	–	–
Rhinolophus sinicus ssp	48	Dakrong NR, Quong Tri, Vietnam	1	–	–	–
		Total	190	107	73	277

NR, Nature Reserve; HND, Hainan Island.

observed patterns of asymmetric gene flow. Body size in bats is particularly useful because it serves as a proxy for genitalia size (Lüpold, Mcelligott & Hosken, 2004). The wing membrane samples were stored in 95% ethanol at –20 °C until genomic DNA was extracted using Qiagen kits. New data were combined with published data from 263 individuals of *R. sinicus* (Mao *et al.*, 2013b) (Fig. 1, Table 1).

DNA SEQUENCING AND ANALYSIS

We amplified and sequenced one mitochondrial (cytochrome *b*; Cyt*b*) and two nuclear genes (the

nucleosome remodelling factor gene *Chd1*, and the short-wavelength-sensitive opsin gene *SWS1*). Sample information for these markers is given in Table 1. Details of primers, polymerase chain reaction (PCR) reactions and the thermal profiles have been described previously (Mao *et al*., 2010b).

For sequencing, we used both primers of each nuclear gene, and the forward primer of *Cytb*. PCR products were run on an ABI PRISM 3700 sequencer (Applied Biosystems). The haplotypes of nuclear gene sequences with multiple heterozygous sites were resolved probabilistically using PHASE, version 2.1 (Stephens, Smith & Donnelly, 2001) implemented in DNASP, version 5 (Librado & Rozas, 2009). The sequences were aligned using CLUSTAL X, version 1.83 (Thompson *et al*., 1997) and edited by eye with BIOEDIT, version 7.0.0 (Hall, 1999). New sequences were deposited in GenBank (accession numbers: JX502488–JX502533).

Phylogenetic trees and networks

To test for possible introgression among *R. s. sinicus*, *R. s. septentrionalis*, and *R. thomasi*, we undertook tree- and network-based phylogenetic reconstructions, and examined these for discordance with respect to each other and with species relationships. Phylogenetic trees were reconstructed using Bayesian inference (BI) in MrBayes, version 3.1.2 (Ronquist & Huelsenbeck, 2003). A congeneric species (*R. affinis*; accession number: FJ185185) was used as an outgroup. The best-fit substitution models were determined by MODELTEST, version 3.0 (Posada & Crandall, 1998) as HKY + G [G = 0.092] for *Cytb*, HKY for *Chd1*, and TVM + I + G (I = 0.748 and G = 0.685) for *SWS1*. For BI, we conducted two simultaneous runs of Metropolis-coupled Markov chain Monte Carlo (MCMC) analysis with the substitution model parameters, each comprising four chains and ten million generations. Trees and parameters were sampled every 100 generations, and the first 25% of the sampled trees were discarded as burn-in. To complement these trees, statistical parsimony network analyses were performed for each of the three genes using TCS, version 1.21 (Clement, Posada & Crandall, 2000).

To test for historical mtDNA introgression among taxa in the wider *rouxii*-group, we repeated the BI tree reconstruction but with the addition of published *Cytb* sequences from these and other horseshoe bat species (accession numbers: AF406806, DQ297575, EU075016, FJ185185–88, FJ185190–93, FJ185197–99, FJ185201, FJ185203–10, FJ185212–15, HM590030–40, HM590046–50, GQ257315–16, GQ257337, GQ257363, JQ316201–06, JQ316208–14). Four *Hipposideros* species and *Megaderma lyra* (accession numbers: DQ054808, EU934483–84, FJ185182–83, DQ888678) were used as outgroups. The best-fit substitution model was determined by MODELTEST as TVM + I + G (I = 0.499 and G = 1.019) and all other settings remained the same as before.

Demographic analysis

Because introgression often follows a population expansion, we inferred demographic histories by plotting mismatch distributions for *Cytb* dataset using ARLEQUIN, version 3.0 (Excoffier, Laval & Schneider, 2005). Where an expansion model could not be rejected, we estimated the timing of expansion (t) based on tau = $2ut$, where u is the mutation rate per locus per generation. We converted the scaled time into years using a sequence divergence rate of 4% per Myr (Hulva *et al*., 2004) and a generation time of 2 years (Flanders *et al*., 2009).

Introgression or incomplete lineage sorting

In cases where we detected closely-related or identical gene haplotypes shared between taxa (see Results), we determined the relative role of gene flow (i.e. introgression) and incomplete lineage sorting of the ancestral polymorphism using isolation-with-migration (IM) models implemented in the software IM (Hey & Nielsen, 2004). The model assumes panmixia within samples and also assumes that markers are neutral and not subject to recombination. Recent studies have shown that population structure has little effect on IM model parameter estimates, except for estimates of population divergence time (Strasburg & Rieseberg, 2011). Here, we only consider the estimates of migration rates between populations. Recombination was tested by calculating the minimum number of recombination events (R_m) in DNASP and only sections without recombination were used in analyses. The Hudson–Kreitman–Aguade test (Hudson, Kreitman & Aguade, 1987) was conducted in DNASP to check for neutrality, which was not significant for each pairwise comparison of markers.

IM analyses were performed on two datasets: mtDNA (*Cytb*) and combined ncDNA (*Chd1* and *SWS1*). To incorporate the differences in effective population size among markers, we set inheritance scalars as: 0.25 for *Cytb* and 1 for *Chd1* and *SWS1*. We estimated the scaled directional migration rate ($m_1 = m_1/u$ and $m_2 = m_2/u$; where u is mutation rate per locus per year) between *R. s. septentrionalis* and the newly-sampled *R. thomasi*, and also between a possible new taxon and *R. s. sinicus* in the east (see Results). Gene flow between *R. s. septentrionalis* and

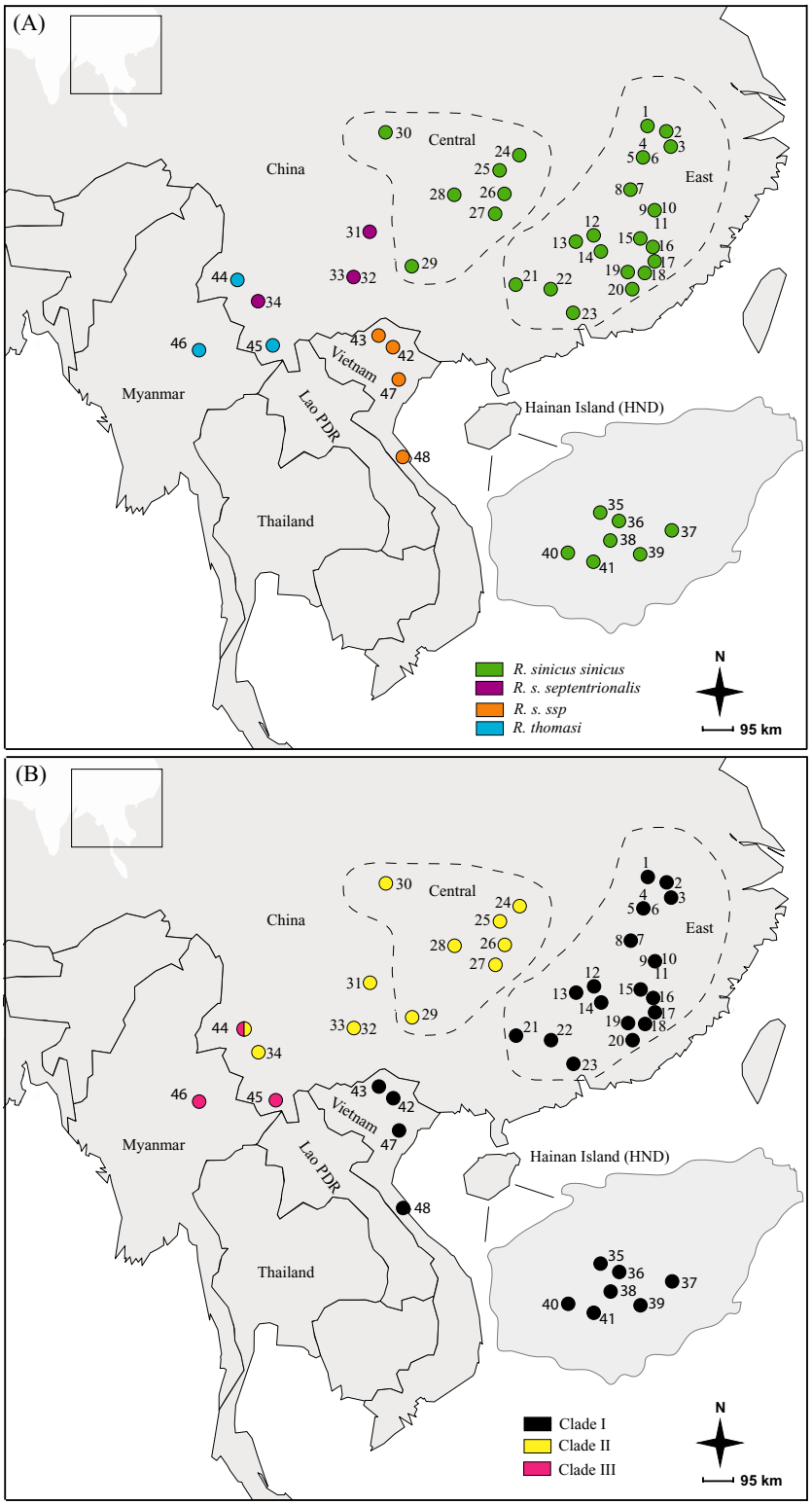
(A)
China
Central
East
Myanmar
Vietnam
Lao PDR
Thailand
Hainan Island (HND)
R. sinicus sinicus
R. s. septentrionalis
R. s. ssp
R. thomasi
N
95 km
(B)
China
Central
East
Myanmar
Vietnam
Lao PDR
Thailand
Hainan Island (HND)
Clade I
Clade II
Clade III
N
95 km

Figure 1. Map showing the sampling sites, modified from Mao *et al*. (2013b), with corresponding membership of taxa and mitochondrial (mt)DNA clades for each population. A, populations are coloured by taxon membership: *Rhinolophus sinicus sinicus* (green), *Rhinolophus sinicus septentrionalis* (purple), *Rhinolophus thomasi* (blue) and *Rhinolophus sinicus ssp* (orange). Numbers indicate the sampling locality in accordance with Table 1. B, populations are presented as pie charts in which individuals are coloured based on the membership of mtDNA clades: clade I (black), clade II (yellow), and clade III (red). In both maps, the two mainland groups of *R. s. sinicus* (i.e. Central and East) are indicated by broken lines.

R. s. sinicus has been investigated previously (Mao *et al*., 2013b). The starting values of prior distributions were determined by allowing large parameter intervals in several preliminary runs. Three final runs were conducted with different random seeds and a single chain with 2×10^8 iterations following a burn-in of 10^7 steps. Each run included five MCMCs with ten multiple chain-swapping attempts.

Microsatellite-based analyses of recent gene flow

To test whether observed patterns of discordance between mtDNA and ncDNA datasets (see Results) could be explained by recent gene flow, we also performed analyses of population structure using microsatellite data. For this, new samples were genotyped at eight microsatellites *sensu* Mao *et al*. (2013b). PCR products were visualized on an ABI 3730 sequencer and analyzed with GENEMAPPER, version 3.7 (ABI). We checked for possible null alleles and genotyping errors using MICRO-CHECKER, version 2.2.3 (Van Oosterhout *et al*., 2004) and used GENEPOP, version 3.4 (Raymond & Rousset, 1995) to test for deviation from Hardy–Weinberg equilibrium and linkage equilibrium at each locus within each taxon. New genotype data were combined with existing genotype data from *R. sinicus* (Mao *et al*., 2013b). To test for population structure, we used STRUCTURE, version 2.2 (Pritchard, Stephens & Donnelly, 2000) to assign individuals to increasing numbers of clusters (K). At each K, we performed ten replicate runs (10^6 iterations with an initial burn-in of 10^5 iterations each run) based on the admixture model. Similar replicate runs were grouped based on a symmetric similarity coefficient of > 0.9 using CLUMPP (Jakobsson & Rosenberg, 2007) and visualized using DISTRUCT, version 1.1 (Rosenberg, 2004). The level of recent gene flow among taxa was further assessed by estimating the number of putative first-generation migrants using the method of Rannala & Mountain (1997), implemented in GENECLASS, version 2.0 (Piry *et al*., 2004). The probability to exclude an individual from the reference population was calculated with 1000 simulated individuals and a threshold of 0.01 (Paetkau *et al*., 2004).

RESULTS

Morphological data

Comparisons of forearm data (Fig. 2) revealed that *thomasi* was significantly smaller than *septentrionalis* ($t = -6.144$, d.f. = 61, $P < 0.01$) but did not differ in size from *sinicus* ($t = 0.524$, d.f. = 40, $P > 0.05$), and that *sinicus* was significantly smaller than *septentrionalis* ($t = -7.536$, d.f. = 81, $P < 0.01$). However, previous examination of skull and nose-leaf size revealed *R. thomasi* to be distinct from both other taxa (Bates *et al*., 2004). More unexpectedly, the newly-sampled bats from Vietnam initially identified as *R. s. sinicus* also showed subtle morphological differences from *R. s. sinicus* and *R. thomasi* (V. Thong, unpubl. data). On the basis of these morphological examinations and also on genetic data (see below), we speculate that a cryptic distinct subspecies or species from Vietnam could be present and, therefore, we hereafter refer to these bats as *R. s. ssp*.

Phylogenetic trees and networks

We aligned new *Cytb* sequences from bats sampled in China, Vietnam, and Myanmar with existing *Cytb* sequences from 166 *R. sinicus* sampled from across mainland China and Hainan Island (GenBank accession numbers: JN650674–JN650839) and one *R. thomasi* from Myanmar (FJ85215). The final *Cytb* alignment (465 bp) contained 70 haplotypes with 86 polymorphic sites, including 49 haplotypes from *R. s. sinicus*, four from *R. s. septentrionalis*, eight from *R. thomasi*, one shared between *R. s. septentrionalis* and *R. thomasi*, and eight from *R. s. ssp*. Phylogenetic reconstruction using Bayesian methods recovered three well supported clades (i.e. clades I, II, and III) (Fig. 3A). Clade I contained all *R. s. sinicus* from east China and Hainan and all individuals of *R. s. ssp*. Clade II contained *R. s. sinicus* and *R. s. septentrionalis* from central mainland China, as well as two haplotypes (haplotypes 8 and 9) of *R. thomasi* from location 44 (Fig. 1) of which haplotype 8 was also shared with *R. s. septentrionalis*. Clade III contained only *R. thomasi* haplotypes. Consistent with the tree result, a network reconstruction of *Cytb* sequences recovered three subnetworks with a connection limit of 18 mutation steps, corresponding well to clades I, II, and III (Fig. 3B).

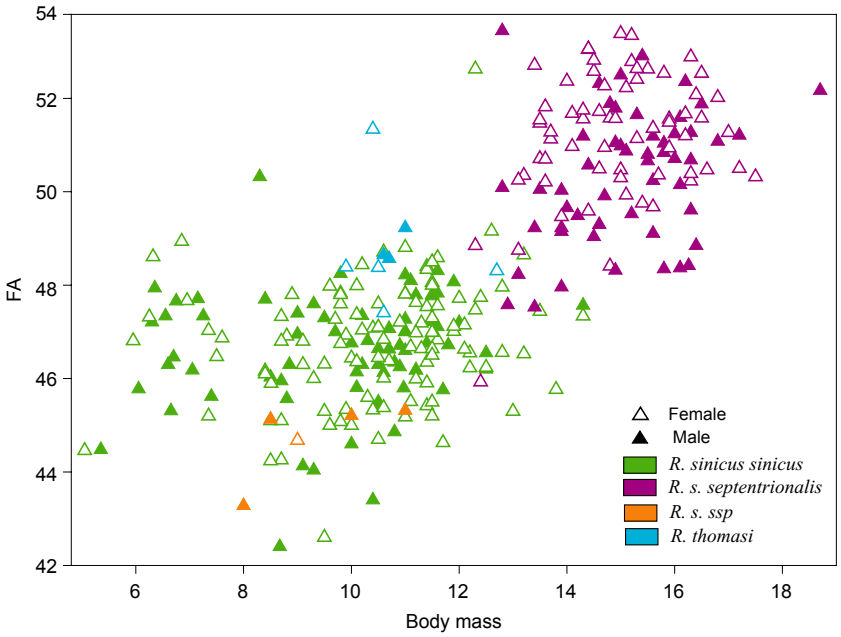

Figure 2. Morphological measurements of forearm (FA; mm) and body mass (g). Measurement data of *Rhinolophus sinicus* individuals were obtained from Mao *et al*. (2013b). Open and filled triangles correspond to female and male bats, respectively. Individuals are coded by taxon membership, as in Fig. 1A.

Figure 3. Phylogenetic trees and statistical parsimony networks based on mitochondrial DNA and nuclear markers. A, Bayesian inference (BI) tree based on *Cytb* haplotypes. Clades are colour-coded with bars in accordance with Fig. 1B. The shared haplotype (Hap 8) between *Rhinolophus sinicus septentrionalis* and *Rhinolophus thomasi* is shown in black. B, statistical parsimony network for *Cytb* haplotypes. C, BI tree and statistical parsimony network for *Chd1*. The tree was rooted with *Rhinolophus affinis* (not shown). A 10-bp deletion (i.e one mutational step) between hap10 and hap6 is also shown by an arrow. D, BI tree and statistical parsimony network for *SWS1*. The tree was rooted with *R. affinis* (not shown). Node support in the BI trees is indicated with Bayesian posterior probabilities. Each circle in the networks represents a single haplotype and the area of circle size is scaled by haplotype frequency. Filled black circles represent missing or unsampled haplotypes. Numbers in the network of *Cytb* denote mutational steps. Haplotypes are coloured by taxon membership, as in Fig. 1A.

We sequenced two nuclear genes (*Chd1* and *SWS1*) for a subset of samples of *R. thomasi* and *R. s. ssp* (Table 1). New *Chd1* sequences combined with previous data from *R. sinicus* (accession numbers: JN650840–JN650949) gave an alignment that contained ten haplotypes with nine polymorphic sites and 12 indels. The BI tree and network of *Chd1* haplotypes exhibited three clades and three subnetworks, broadly corresponding to *R. s. septentrionalis*, *R. s. sinicus* + *R. thomasi*, and *R. s. ssp*, respectively (Fig. 3C). One sequence (*R. thomasi* from location 44) had two heterozygous sites whose haplotypes were resolved with a probability of over 0.8. Of the two *Chd1* haplotypes of this individual, one clustered with *R. s. septentrionalis* and the other with *R. thomasi* (Fig. 3C).

New *SWS1* sequences combined with existing data from *R. sinicus* (accession numbers: JN650950–JN651016) gave an alignment containing 41 haplotypes with 36 polymorphic sites and 17 indels. By contrast to *Chd1*, the BI tree and network of *SWS1* resolved two clades and two subnetworks, broadly corresponding to *R. s. septentrionalis* + *R. thomasi* + *R. s. ssp*, and *R. s. sinicus*, respectively (Fig. 3D). One exception was from a haplotype of *R. s. sinicus* that clustered with *R. s. septentrionalis*.

A Bayesian phylogeny of *Cytb* sequences obtained from 27 *Rhinolophus* taxa plus outgroups confirmed a sister subspecies relationship between *R. s. sinicus* and *R. s. septentrionalis*, with newly sampled bats from Vietnam (*R. s. ssp*) clustering with the former. Phylogenetic reconstruction also confirmed the well-supported sister species relationship between *R. sinicus* and *R. thomasi*. However, contrary to expectations, these three taxa formed a moderately well supported clade (Bayesian posterior

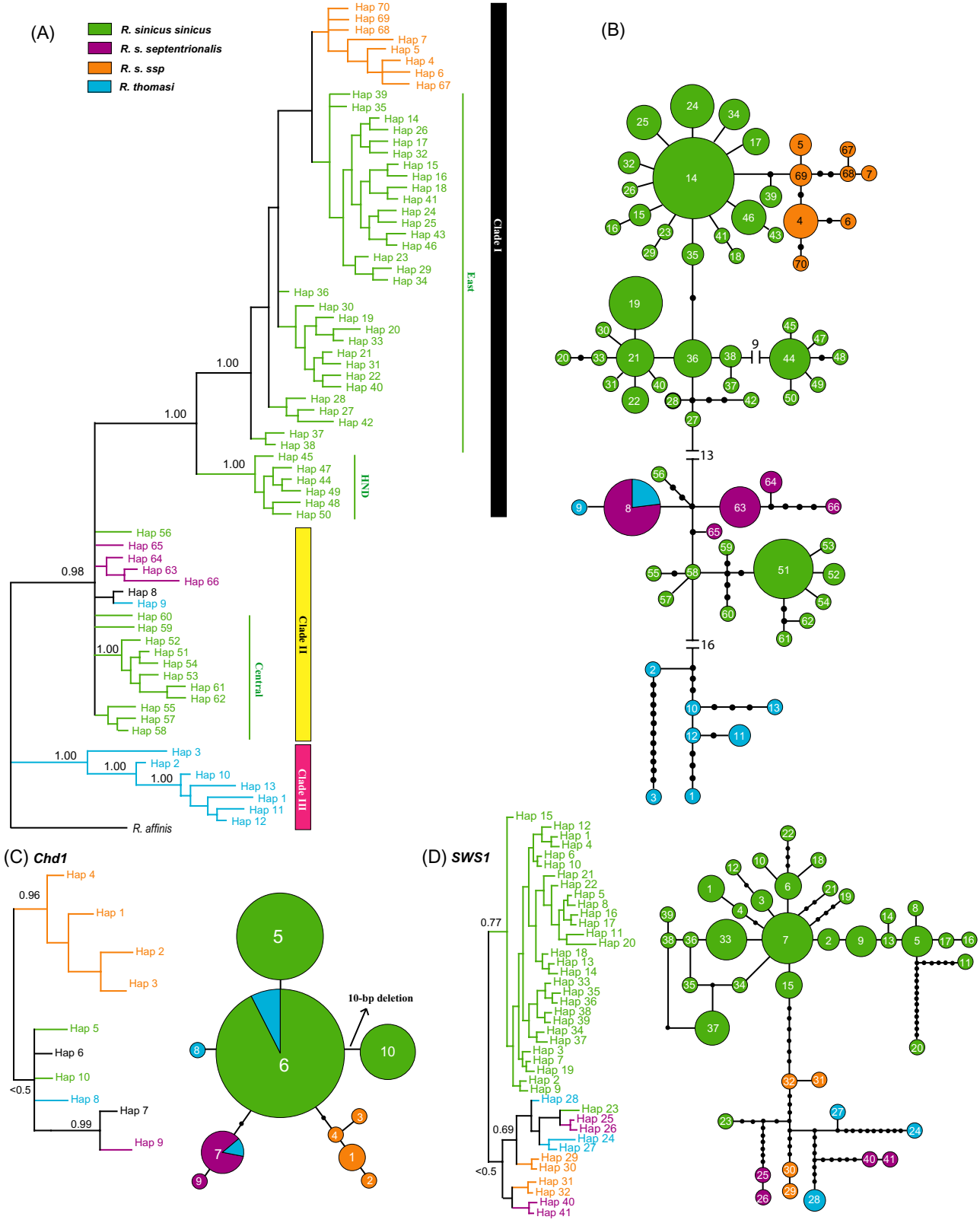
(A)
R. sinicus sinicus
R. s. septentrionalis
R. s. ssp
R. thomasi
Hap 70
Hap 69
Hap 68
Hap 7
Hap 5
Hap 4
Hap 6
Hap 67
Hap 39
Hap 35
Hap 14
Hap 26
Hap 17
Hap 32
Hap 15
Hap 16
Hap 18
Hap 41
Hap 24
Hap 25
Hap 43
Hap 46
Hap 23
Hap 29
Hap 34
Hap 36
Hap 30
Hap 19
Hap 20
Hap 33
Hap 21
Hap 31
Hap 22
Hap 40
Hap 28
Hap 27
Hap 42
Hap 37
Hap 38
Hap 45
Hap 47
Hap 44
Hap 49
Hap 48
Hap 50
Hap 56
Hap 65
Hap 64
Hap 63
Hap 66
Hap 8
Hap 9
Hap 60
Hap 59
Hap 52
Hap 51
Hap 54
Hap 53
Hap 61
Hap 62
Hap 55
Hap 57
Hap 58
Hap 3
Hap 2
Hap 10
Hap 13
Hap 1
Hap 11
Hap 12
R. affinis
1.00
1.00
1.00
1.00
0.98
1.00
1.00
1.00
East
HND
Central
Clade I
Clade II
Clade III
(B)
(C) Chd1
Hap 4
Hap 1
Hap 2
Hap 3
Hap 5
Hap 6
Hap 10
Hap 8
Hap 7
Hap 9
0.96
<0.5
0.99
10-bp deletion
(D) SWS1
Hap 15
Hap 12
Hap 1
Hap 4
Hap 6
Hap 10
Hap 21
Hap 22
Hap 5
Hap 8
Hap 16
Hap 17
Hap 11
Hap 20
Hap 18
Hap 13
Hap 14
Hap 33
Hap 35
Hap 36
Hap 38
Hap 39
Hap 34
Hap 37
Hap 3
Hap 7
Hap 19
Hap 2
Hap 9
Hap 28
Hap 23
Hap 25
Hap 26
Hap 24
Hap 27
Hap 29
Hap 30
Hap 31
Hap 32
Hap 40
Hap 41
0.77
0.69
<0.5

Figure 4. Bayesian inference tree based on cytochrome *b* sequences of *Megaderma lyra*, 4 *Hipposideros*, and 27 *Rhinolophus* species. Node support is indicated with the Bayesian posterior probability.

probability = 0.74) with other horseshoe bat species to the exclusion of the other currently recognized members of the *rouxii*-group (*R. rouxii* and *R. indorouxii*) (Fig. 4). In addition to our focal taxa, we also noted the unexpected placement of individual haplotypes of *R. monoceros* (accession number: FJ185209) and *R. stheno* (accession number: FJ185213), suggesting possible problems with museum identifications or sample handling (Fig. 4).

Demographic analysis

Our demographic analyses based on mismatch distributions could not reject the model of population expansion for *R. thomasi* and *R. s. ssp* [SSD (the sum of square deviations) *P*-value > 0.05]. The inferred expansion time for these two taxa is similar [i.e. 130 000 years BP (95% confidence interval = 34 000–296 000 years BP) for *R. thomasi* and 150 000 years BP (95% confidence interval = 31 000–403 000 years BP) for *R. s. ssp*]. These results are therefore consistent with an episode of demographic growth, a condition that is frequently linked to asymmetric introgression of neutral genes.

Introgression or incomplete lineage sorting

Three independent IM runs were found to be consistent and produced similar posterior distributions with the effective sample sizes of > 500 for all parameters. Here, we only consider the estimates of migration rate for which the posterior probability distributions showed clear peaks and bounds within the prior distributions (Fig. 5). The posterior modes with 90% credible intervals are shown in Figure 5. The results of the IM analysis for mtDNA revealed a significant level of gene flow from *R. s. septentrionalis* to *R. thomasi*, whereas no gene flow was detected in the opposite direction. Consistent with this asymmetric mtDNA introgression, additional IM analysis of combined ncDNA sequences also showed evidence of considerable nuclear gene flow from *R. s. septentrionalis* to *R. thomasi* (Fig. 5). By contrast, IM analyses of mtDNA revealed no gene flow between the eastern population of *R. s. sinicus* and the putative new taxon *R. s. ssp* in either direction and, although nuclear gene flow was detected for combined ncDNA sequences, this is probably unreliable as a result of the almost flat posterior probability distribution (Fig. 5).

Microsatellite-based analyses of recent gene flow

Microsatellite data showed no evidence of null alleles or a significant departure from Hardy–Weinberg equilibrium and linkage equilibrium after Bonferroni correction, with the exception of one marker that showed deviation from Hardy–Weinberg equilibrium in *R. thomasi*. Clustering analysis in STRUCTURE was performed for all individuals and, consistent with the previous study (Mao *et al.*, 2013b), individuals of eastern populations of *R. s. sinicus* were firstly separated from others at $K = 2$ (Fig. 6A). Subsequent clustering analyses of samples that clustered together at $K = 2$ showed that individuals of *R. s. septentrionalis* and *R. thomasi* continued to group together at $K = 2$, 3, and 4 (Fig. 6B), thus consistent with the scenario of nuclear introgression suggested by ncDNA sequence data. Individuals of *R. s. ssp* clustered with some individuals of eastern *R. s. sinicus* at values of K from 2 to 5, after which they separated (Fig. 6B). No first-generation migrants were detected by GENECLASS either between *R. s. septentrionalis* and *R. thomasi*, or between *R. s. sinicus* and *R. s. ssp*.

DISCUSSION

We obtained new genetic and morphology datasets and combined these with published data to test for the extent of gene flow between *R. sinicus* and *R. thomasi.* We confirmed the sister relationship between recognized pairs of subspecies and of species; however, wider phylogenetic reconstruction showed that these two species (*R. sinicus* and *R. thomasi*) are unlikely to be close relatives of *R. rouxii* (Fig. 4). This finding was unexpected and disagrees with current horseshoe bat systematics, probably reflecting the fact that, to our knowledge, previous studies have not included genetic data from all three species at the same time (Stoffberg *et al.*, 2010; Chattopadhyay *et al.*, 2012). Although available genetic data for *R. rouxii* and *R. indorouxii* were limited to *Cytb* sequences, and thus more markers are needed, we suggest that these bats are in need of systematic revision and that the current grouping based on taxonomy is probably erroneous and confounded by phenotypic convergence.

Discordance between mitochondrial and nuclear datasets

Conflicts between mitochondrial and nuclear datasets can occur as a result of introgression as well as

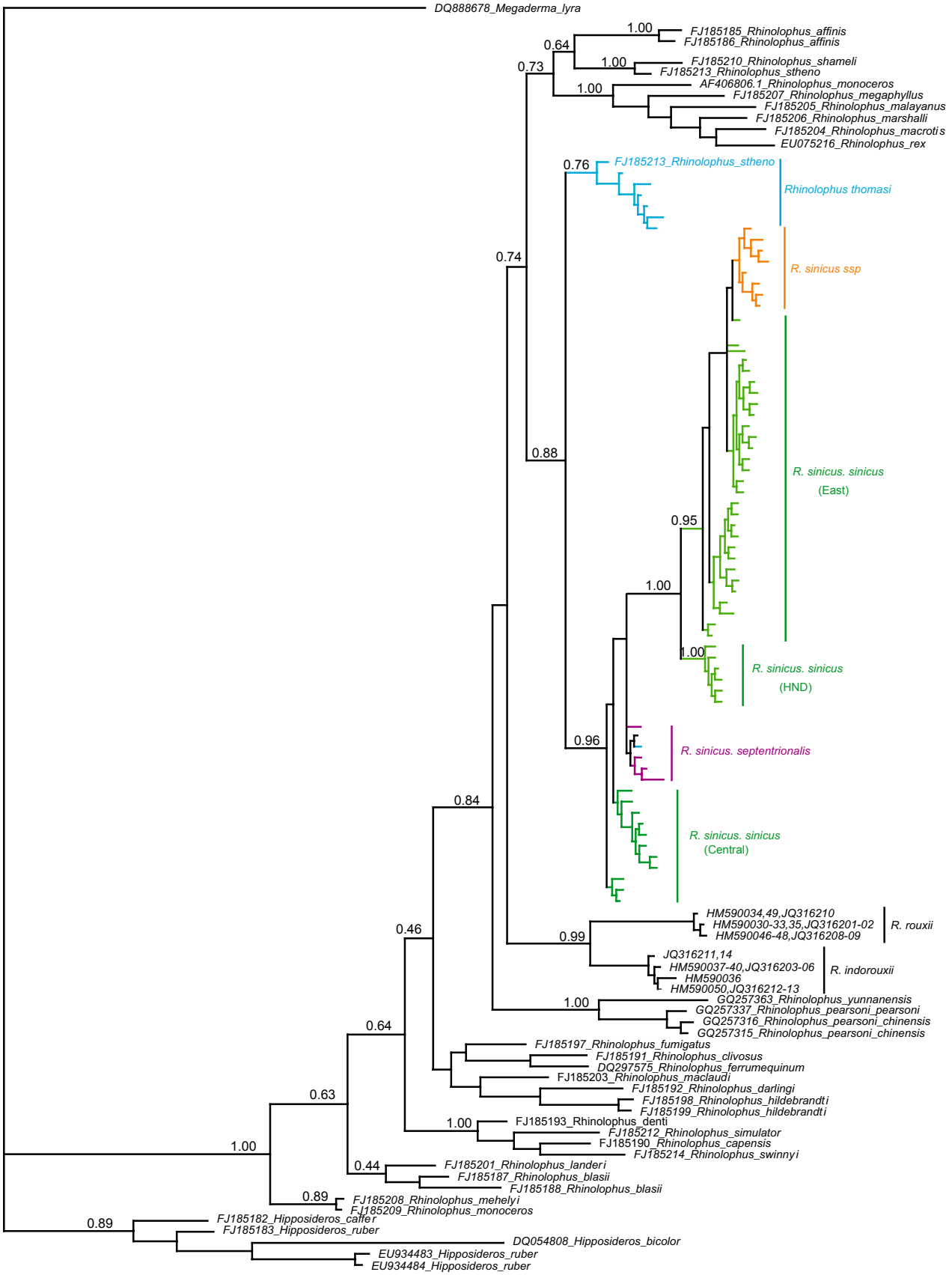
DQ888678_Megaderma_lyra
1.00
FJ185185_Rhinolophus_affinis
FJ185186_Rhinolophus_affinis
0.64
0.73
1.00
FJ185210_Rhinolophus_shameli
FJ185213_Rhinolophus_stheno
1.00
AF406806.1_Rhinolophus_monoceros
FJ185207_Rhinolophus_megaphyllus
FJ185205_Rhinolophus_malayanus
FJ185206_Rhinolophus_marshalli
FJ185204_Rhinolophus_macrotis
EU075216_Rhinolophus_rex
0.76
FJ185213_Rhinolophus_stheno
Rhinolophus thomasi
0.74
R. sinicus ssp
0.88
R. sinicus. sinicus
(East)
0.95
1.00
1.00
R. sinicus. sinicus
(HND)
0.96
R. sinicus. septentrionalis
0.84
R. sinicus. sinicus
(Central)
HM590034,49,JQ316210
HM590030-33,35,JQ316201-02
HM590046-48,JQ316208-09
R. rouxii
0.46
0.99
JQ316211,14
HM590037-40,JQ316203-06
HM590036
HM590050,JQ316212-13
R. indorouxii
1.00
GQ257363_Rhinolophus_yunnanensis
GQ257337_Rhinolophus_pearsoni_pearsoni
GQ257316_Rhinolophus_pearsoni_chinensis
GQ257315_Rhinolophus_pearsoni_chinensis
0.64
FJ185197_Rhinolophus_fumigatus
FJ185191_Rhinolophus_clivosus
DQ297575_Rhinolophus_ferrumequinum
FJ185203_Rhinolophus_maclaudi
0.63
FJ185192_Rhinolophus_darlingi
FJ185198_Rhinolophus_hildebrandti
FJ185199_Rhinolophus_hildebrandti
1.00
FJ185193_Rhinolophus_denti
FJ185212_Rhinolophus_simulator
1.00
FJ185190_Rhinolophus_capensis
FJ185214_Rhinolophus_swinnyi
0.44
FJ185201_Rhinolophus_landeri
FJ185187_Rhinolophus_blasii
FJ185188_Rhinolophus_blasii
0.89
FJ185208_Rhinolophus_mehelyi
FJ185209_Rhinolophus_monoceros
0.89
FJ185182_Hipposideros_caffer
FJ185183_Hipposideros_ruber
DQ054808_Hipposideros_bicolor
EU934483_Hipposideros_ruber
EU934484_Hipposideros_ruber

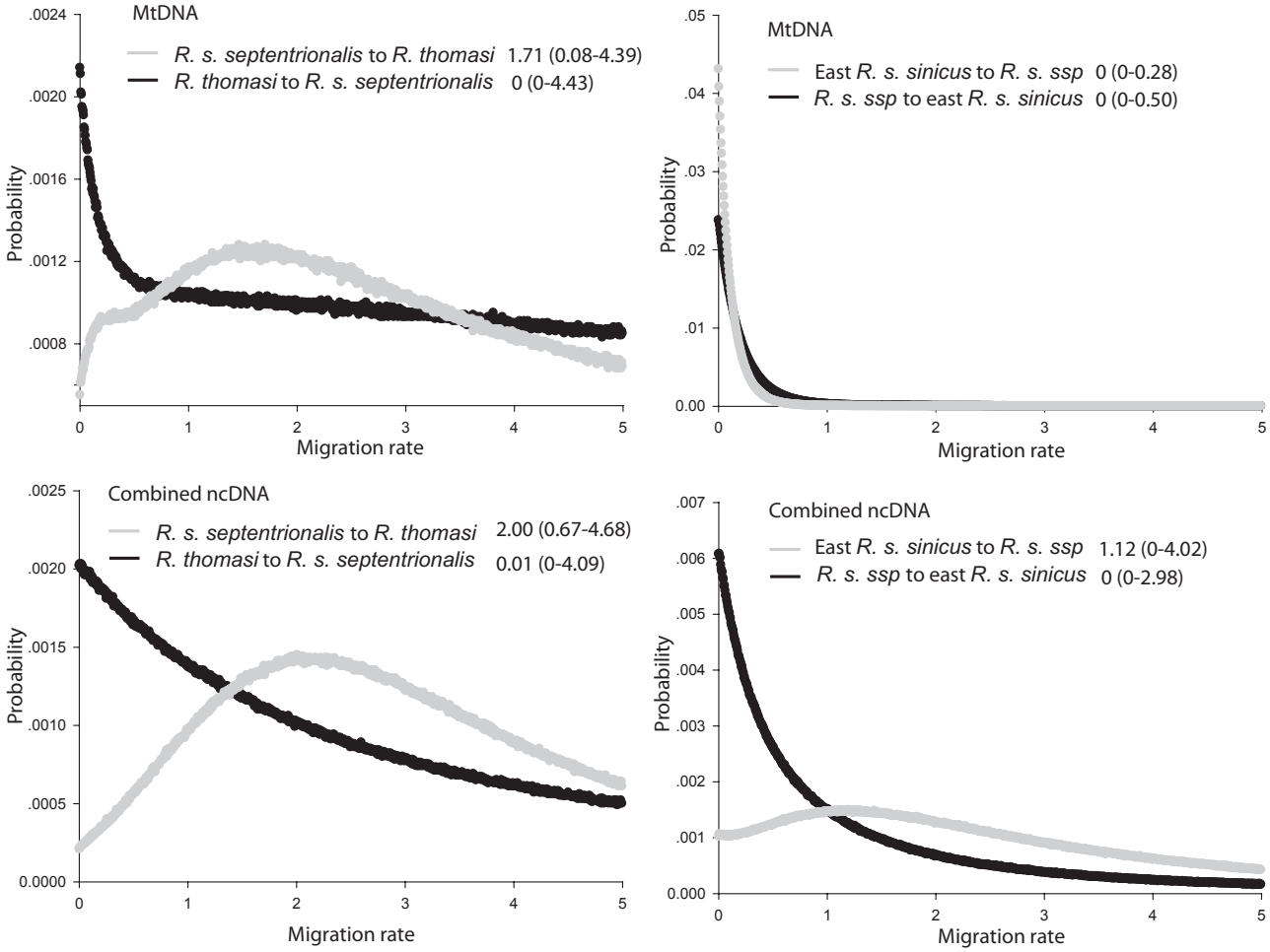

Figure 5. Marginal posterior probability distributions of migration rates between *Rhinolophus sinicus septentrionalis* and *Rhinolophus thomasi*, and between *Rhinolophus sinicus ssp* and eastern *Rhinolophus sinicus sinicus*. Isolation-with-migration (IM) analysis was performed based on mitochondrial DNA and combined nuclear DNA, respectively. The IM estimates of posterior mode and 90% credible intervals for directional migration rates (m_1 and m_2) are also shown. Maximum-likelihood estimates of migration rates of < 0.0050 are shown as 0 (Nielsen & Wakeley, 2001).

incomplete lineage sorting of ancestral polymorphism (Funk & Omland, 2003; Ballard & Whitlock, 2004). Although coalescent-based models (Nielsen & Wakeley, 2001) have been developed to distinguish these alternatives, this task remains difficult (Hey & Nielsen, 2004). In the present study, at least three cases of discordance between different sources of data were observed.

First, mtDNA haplotypes of central *R. s. sinicus* showed a closer relationship with those of *R. s. septentrionalis* in the adjacent region than with ones of *R. s. sinicus* further east (Figs 1B and 3A), whereas analyses of nuclear genes and microsatellites revealed a clear separation between these two subspecies (Mao *et al*., 2013b; present study). Note that this mtDNA introgression was asymmetric from *R. s. septentrionalis* to central *R. s. sinicus* with zero gene flow in the reverse direction (Mao *et al*., 2013b).

Second, at the species level, although mtDNA haplotypes of *R. thomasi* and *R. s. septentrionalis* were broadly reciprocally monophyletic, two mtDNA haplotypes of the former clustered with the latter and one haplotype was shared, which could be best explained by mtDNA introgression between these two taxa. Indeed, the IM analysis for mtDNA revealed significant gene flow from *R. s. septentrionalis* to *R. thomasi.* An alternative scenario (i.e. incomplete lineage sorting) is less likely in this case because introgressed haplotypes were not seen across the ranges (Coyne & Orr, 2004) but, instead, were recorded within an area of range overlap (i.e. location 44) (Fig. 1). Conflicts were also observed between mtDNA/species identities and ncDNA; specifically, a *SWS1* network suggested *R. thomasi* had a closer relationship with *R. s. septentrionalis* than with *R. s. sinicus*, and nuclear introgression between *R. s.*

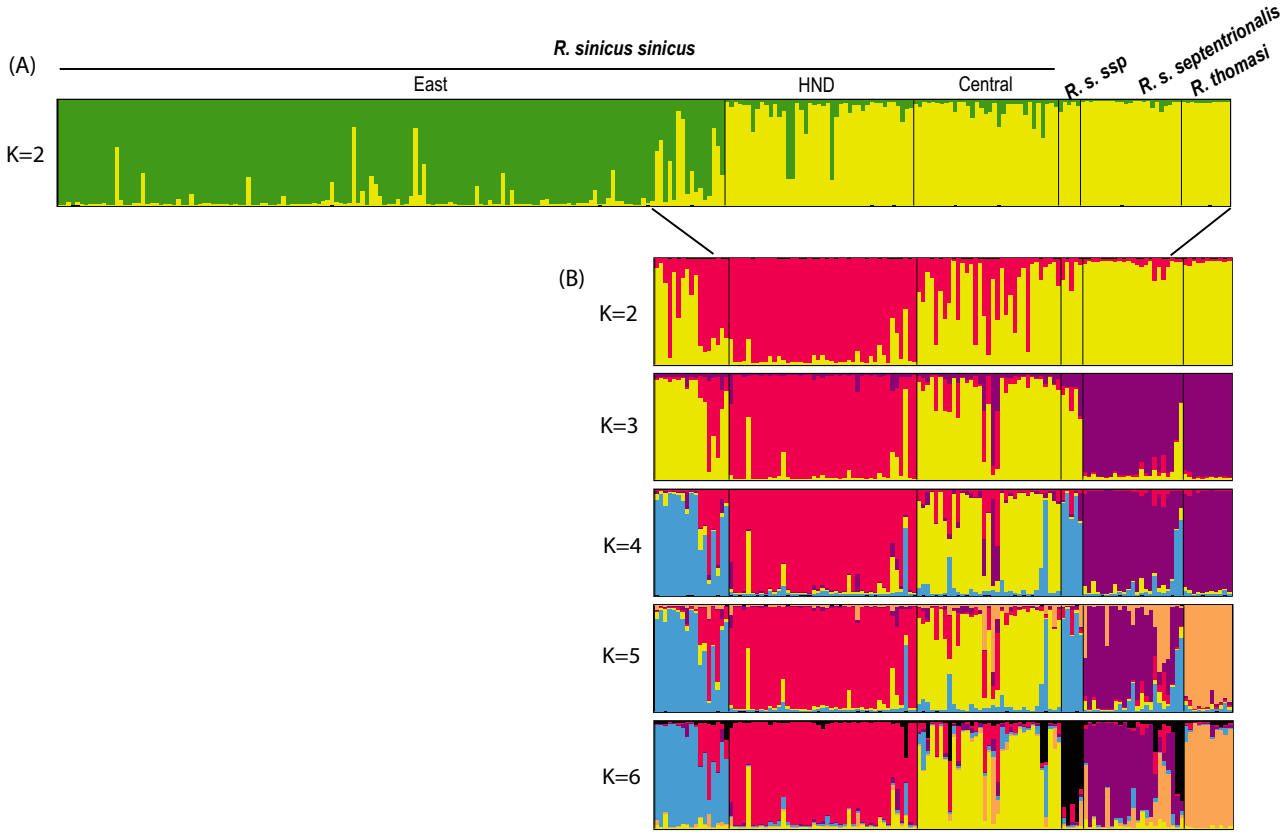

Figure 6. Clustering of individuals in STRUCTURE based on microsatellite genotypes. A, clustering of all individuals of *Rhinolophus sinicus*, *Rhinolophus thomasi*, and *Rhinolophus sinicus ssp* based on eight microsatellite loci in STRUCTURE for $K = 2$. B, further clustering of those individuals that clustered together in (A) for K from 2 to 6. Each bar corresponds to one individual and the colour of each bar represents the probability of an individual to clusters.

septentrionalis and *R. thomasi* was supported by the IM analysis of the combined *Chd1* and *SWS1* data. By contrast, sequences of *Chd1* revealed a clear separation between most *R. thomasi* and *R. s. septentrionalis*. For one individual of *R. thomasi* from location 44, the assignment of its two *Chd1* alleles to *R. thomasi* and *R. s. septentrionalis* and of its mtDNA to *R. s. septentrionalis* suggests that it was a possible F_1 hybrid between a *R. thomasi* male and a *R. s. septentrionalis* female. In agreement with the results of nuclear genes, the STRUCTURE analysis of microsatellites revealed that individuals of *R. s. septentrionalis* and *R. thomasi* clustered together at increasing values of K from 2 to 4; however, no first-generation migrants were detected between these two taxa, perhaps suggesting gene flow probably occurred in the past.

The third instance of discordance was seen in the relationship between *R. s. sinicus* and a putative new taxon identified in the present study referred to as *R. s. ssp*. mtDNA tree and network reconstructions showed individuals of *R. s. ssp* to be part of eastern *R. s. sinicus*; however, networks of nuclear genes and clustering of microsatellites both revealed the clear separation between these two taxa, which also supported the morphological data that suggested the possible presence of an independent taxon. Once again, incomplete lineage sorting offers a less satisfactory explanation in this case because of the faster coalescence time of mtDNA compared to that of ncDNA (Palumbi, Cipriano & Hare, 2001). Nonetheless, the IM analysis for mtDNA detected zero gene flow between these two taxa. This discrepancy could arise if the assumptions of the IM models are violated; for example, if unsampled populations are contributing to introgression (Hey & Nielsen, 2004). We also cannot rule out the possibility that gene flow between eastern *R. s. sinicus* and *R. s. ssp* occurs via an intermediate that is either unsampled or extinct (Melo-Ferreira *et al*., 2007; Renoult *et al*., 2009).

Mechanisms for asymmetric introgression of mtDNA

Perhaps the most striking finding in the present study is that mtDNA introgression has occurred

asymmetrically in both cases, from *R. s. septentrionalis* to *R. thomasi*, and from *R. s. septentrionalis* to *R. s. sinicus*. Strong asymmetric mtDNA introgression may reflect a propensity of matings between *R. s. septentrionalis* females and the males of the other taxa. Currently, there are no available data of mating behaviour in this species complex, although asymmetric mating between the sexes has been reported in other systems (Shaw & Lugo, 2001; Stein & Uy, 2006). Mechanical factors in prezygotic isolation could reflect size differences or differences in genital morphology (Sota & Kubota, 1998; Hosken & Stockley, 2004). Indeed, a genital 'lock and key' system as a mechanical barrier has been reported in other taxa (Coyne & Orr, 2004). Among our focal taxa, it is noteworthy that *R. s. septentrionalis* has a much larger body size and mass than either *R. thomasi* or *R. s. sinicus* (Fig. 2) and, thus, if genital size scales with body size then an asymmetric mismatch in genitalia could be a determinant of the direction of mtDNA introgression (Hosken & Stockley, 2004; Nagata *et al*., 2007). Indeed, genital size is positively associated with male body size and relative body mass in the noctule bat (*Nyctalus noctula*) where it is assumed to be under directional sexual selection (Lüpold *et al*., 2004). More studies are needed on genital morphology in bats in order to clarify its importance in contributing to reproduction isolation among taxa.

The observed asymmetric mtDNA introgression among horseshoe bats could have arisen as a result of other alternative processes. First, range expansions can also lead to the unidirectional spread of neutral genes, which are predicted to flow from the local taxon to the colonizing taxon (Currat *et al*., 2008; Excoffier *et al*., 2009). However, a population expansion was not detected for the central *R. s. sinicus* (Mao *et al*., 2013b), although it could not be rejected for *R. thomasi*. Alternatively, unidirectional introgression of mtDNA could occur if natural selection strongly favoured particular mitochondrial genes (a scenario proposed to explain the spread of mtDNA in some hare populations; Melo-Ferreira *et al*., 2005) or if a hybrid zone has shifted (Buggs, 2007). However, the three focal taxa in the present study are from similar altitudinal and climatic conditions and so we have no a priori reason to suspect adaptive introgression (Zhang, Fengquan & Jianmin, 2000). Similarly, there is no hybrid zone between *R. s. septentrionalis* and central *R. s. sinicus*, although past hybridization might have occurred between them as a result of range shifts associated with Pleistocene glaciations (McGuire *et al*., 2007; Sŭsnik *et al*., 2007). One mtDNA haplotype was shared between *R. s. septentrionalis* and *R. thomasi*, indicating recent introgression of mtDNA (Strasburg & Rieseberg, 2011) and therefore a hybrid zone may exist in their connected regions, although more samples of *R. thomasi* will be needed to confirm this. In addition, historical samples will also be necessary to investigate whether this hybrid zone (if present) is/was moving across the space.

Conclusions

The present study adds to the growing body of evidence that highlights the importance of combining information across multiple datasets to reliably delimit taxonomic boundaries and infer population histories. Multilocus datasets, together with morphological data, revealed multiple cases of phylogenetic discordance among four taxa in south-east Asia that are best accounted for by periods of interbreeding. Along with studies of other horseshoe bats (Mao *et al*., 2010a, b), all inferred mtDNA introgressions appear to be asymmetric and, although several scenarios have been proposed to explain this pattern, the consistent size differences do point to a possible mechanical barrier caused by a mismatch in genitalia. Such insights into reproductive barriers obtained from morphology and genetic data are especially valuable for bats, such as the focal taxa, given that observations of mating among wild individuals in underground caves are exceedingly difficult.

ACKNOWLEDGEMENTS

We thank Zhang Junpeng, Zhu Guangjian, Weili, Xudong, Meng Fanxing, and Yuan Xinpu for assistance with the field collection in China. We also thank three anonymous reviewers for their helpful comments that improved an earlier version of the manuscript. This work was funded by a grant awarded to S. Zhang under the Key Construction Program of the National '985' Project and '211' Project, and also by BBSRC China Partnering award to GJ and SJR. X Mao was supported by a Marie Curie International Incoming Fellowship and SJR by a Royal Society Fellowship. Vu Dinh Thong was funded by the National Foundation for Science and Technology Development of Vietnam (NAFOSTED, Project 106.11-2012.02); University of Tuebingen (Germany); Project TN3/T07 of the National Program Tay Nguyen III; and the Institute of Ecology and Biological Resources.

REFERENCES

Arnold ML. 1997. *Natural hybridization and evolution*. Oxford: Oxford University Press.

Avise JC. 1994. *Molecular markers, natural history and evolution*. New York, NY: Chapman & Hall.

Avise JC. 2000. *Phylogeography: the history and formation of species*. Cambridge, MA: Harvard University Press.

Bachtrog D, Thornton K, Clark A, Andolfatto P. 2006. Extensive introgression of mitochondrial DNA relative to nuclear genes in the *Drosophila yakuba* species group. *Evolution* **60:** 292–302.

Ballard JWO, Whitlock MC. 2004. The incomplete natural history of mitochondria. *Molecular Ecology* **13:** 729–744.

Barrowclough GF, Zink RM. 2009. Funds enough, and time: mtDNA, nuDNA and the discovery of divergence. *Molecular Ecology* **18:** 2934–2936.

Barton NH. 2001. The role of hybridization in evolution. *Molecular Ecology* **10:** 551–568.

Bates P, Thi MM, Nwe T, Bu SSH, Mie KM, Nyo N, Khaing AA, Aye NN, Oo T, Mackie I. 2004. A review of *Rhinolophus* (Chiroptera: Rhinolophidae) from Myanmar, including three species new to the country. *Acta Chiropterologica* **6:** 23–48.

Buggs RJA. 2007. Empirical study of hybrid zone movement. *Heredity* **99:** 301–312.

Chattopadhyay B, Garg KM, Kumar AKV, Doss DPS, Ramakrishnan U, Kandula S. 2012. Sibling species in South Indian populations of the rufous horse-shoe bat *Rhinolophus rouxii*. *Conservation Genetics* **13:** 1435–1445.

Clement M, Posada D, Crandall KA. 2000. TCS: a computer program to estimate gene genealogies. *Molecular Ecology* **9:** 1657–1660.

Coyne JA, Orr HA. 2004. *Speciation*. Sunderland, MA: Sinauer Associates.

Csorba G, Ujhelyi P, Thomas N. 2003. *Horseshoe bats of the world (Chiroptera: Rhinolophidae)*. Bishop's Castle: Alana Books.

Currat M, Ruedi M, Petit RJ, Excoffier L. 2008. The hidden side of invasions: massive introgression by local genes. *Evolution* **62:** 1908–1920.

Edwards SV, Beerli P. 2000. Perspective: gene divergence, population divergence, and the variance in coalescence time in phylogeographic studies. *Evolution* **54:** 1839–1854.

Excoffier L, Foll M, Petit RJ. 2009. Genetic consequences of range expansions. *Annual Review of Ecology, Evolution and Systematics* **40:** 481–501.

Excoffier L, Laval LG, Schneider S. 2005. ARLEQUIN version. 3.0: an integrated software package for population genetics data analysis. *Evolutionary Bioinformatics Online* **1:** 47–50.

Flanders J, Jones G, Benda P, Dietz C, Zhang SY, Li G, Sharifi M, Rossiter SJ. 2009. Phylogeography of the greater horseshoe bat, *Rhinolophus ferrumequinum*: contrasting results from mitochondrial and microsatellite data. *Molecular Ecology* **18:** 306–318.

Funk DJ, Omland KE. 2003. Species-level paraphyly and polyphyly: frequency, causes, and consequences, with insights from animal mitochondrial DNA. *Annual Review of Ecology, Evolution and Systematics* **34:** 397–423.

Gomes B, Sousa C, Novo M, Freitas FB, Alves R, Côrte-Real AR, Salgueiro P, Donnelly MD, Almeida AP, Pinto J. 2009. Asymmetric introgression between sympatric molestus and pipiens forms of *Culex pipiens* (Diptera: Culicidae) in the Comporta region, Portugal. *BMC Evolutionary Biology* **9:** 262.

Grant BR, Grant PR. 2008. Fission and fusion of Darwin's finches populations. *Philosophical Transactions of the Royal Society of London Series B, Biological Sciences* **363:** 2821–2829.

Hall TA. 1999. BIOEDIT: a user-friendly biological sequence alignment editor and analysis program for Windows 95/98/NT. *Nucleic Acids Symposium Series* **41:** 95–98.

Hey J, Nielsen R. 2004. Multilocus methods for estimating population sizes, migration rates and divergence time, with applications to the divergence of *Drosophila pseudoobscura* and *D. persimilis*. *Genetics* **167:** 747–760.

Hosken D, Stockley P. 2004. Sexual selection and genital evolution. *Trends in Ecology and Evolution* **19:** 87–93.

Hudson RR, Kreitman M, Aguade M. 1987. A test of neutral molecular evolution based on nucleotide data. *Genetics* **116:** 153–159.

Hulva P, Horácek I, Strelkov PP, Benda P. 2004. Molecular architecture of *Pipistrellus pipistrellus*/*Pipistrellus pygmaeus* complex (Chiroptera: Vespertilionidae): further cryptic species and Mediterranean origin of the divergence. *Molecular Phylogenetics and Evolution* **32:** 1023–1035.

Jakobsson M, Rosenberg NA. 2007. CLUMPP: a cluster matching and permutation program for dealing with label switching and multimodality in analysis of population structure. *Bioinformatics* **23:** 1801–1806.

Klymus KE, Humfeld SC, Marshall VT, Cannatella D, Gerhardt HC. 2010. Molecular patterns of differentiation in canyon treefrogs (*Hyla arenicolor*): evidence for introgressive hybridization with the Arizona treefrog (*H. wrightorum*) and correlations with advertisement call differences. *Journal of Evolutionary Biology* **23:** 1425–1435.

Larsen P, Marchán-Rivadeneira M, Baker RJ. 2010. Natural hybridization generates mammalian lineage with species characteristics. *Proceedings of the National Academy of Sciences of the United States of America* **106:** 11447–11452.

Librado P, Rozas J. 2009. DnaSP v5: a software for comprehensive analysis of DNA polymorphism data. *Bioinformatics* **25:** 1451–1452.

Lüpold S, Mcelligott AG, Hosken DJ. 2004. Bat genitalia: allometry, variation and good genes. *Biological Journal of the Linnean Society* **83:** 497–507.

Mallet J, Beltran M, Neukirchen W, Linares M. 2007. Natural hybridization in heliconiine butterflies: the species boundary as a continuum. *BMC Evolutionary Biology* **7:** 28.

Mao XG, He GM, Hua PY. Jones G, Zhang SY, Rossiter SJ. 2013a. Historical introgression and the persistence of ghost alleles in the intermediate horseshoe bat *Rhinolophus affinis*. *Molecular Ecology* **22:** 1035–1050.

Mao XG, He GM, Zhang JP, Rossiter SJ, Zhang SY. 2013b. Lineage divergence and historical gene flow in the Chinese horseshoe bat (*Rhinolophus sinicus*). *PLoS ONE* **8:** e56786.

Mao X, Thong VD, Bates PJJ, Jones G, Zhang S, Rossiter S. 2013c. Data from: Multiple cases of asymmetric introgression among horseshoe bats detected by phylogenetic conflicts across loci. *Dryad Digital Repository*. doi:10.5061/dryad.sd60p.

Mao XG, Zhang JP, Zhang SY, Rossiter SJ. 2010a. Historical male-mediated introgression in horseshoe bats revealed by multi-locus DNA sequence data. *Molecular Ecology* **19:** 1352–1366.

Mao XG, Zhu GJ, Zhang SY, Rossiter SJ. 2010b. Pleistocene climatic cycling drives intra-specific diversification in the intermediate horseshoe bat (*Rhinolophus affinis*) in Southern China. *Molecular Ecology* **19:** 2754–2769.

Maroja LS, Andres JA, Harrison RG. 2009. Genealogical discordance and patterns of introgression and selection across a cricket hybrid zone. *Evolution* **63:** 2999–3015.

Mavárez J, Salazar C, Bermingham E, Salcedo C, Jiggins CD, Linares M. 2006. Speciation by hybridization in *Heliconius* butterflies. *Nature* **441:** 868–871.

McGuire JA, Linkem CW, Koo MS, Hutchison DW, Lappin AK, Orange DI, Lemos-Espinal J, Riddle BR, Jaeqer JR. 2007. Mitochondrial introgression and incomplete lineage sorting through space and time: phylogenetics of crotaphytid lizards. *Evolution* **61:** 2879–2897.

Melo-Ferreira J, Boursot P, Randi E, Kryukov A, Suchentrunk F, Ferrand N, Alves PC. 2007. The rise and fall of the mountain hare (*Lepus timidus*) during Pleistocene glaciations: expansion and retreat with hybridization in the Iberian Peninsula. *Molecular Ecology* **16:** 605–618.

Melo-Ferreira J, Boursot P, Suchentrunk F, Ferrand N, Alves PC. 2005. Invasion from the cold past: extensive introgression of mountain hare (*Lepus timidus*) mitochondrial DNA into three other hare species in Northern Iberia. *Molecular Ecology* **14:** 2459–2464.

Morgan K, Linton Y-M, Somboon P, Saikia P, Dev V, Socheat D, Walton C. 2010. Inter-specific gene flow dynamics during the Pleistocene-dated speciation of forest-dependent mosquitoes in Southeast Asia. *Molecular Ecology* **19:** 2269–2285.

Nagata N, Kubota K, Yahiro K, Sota T. 2007. Mechanical barriers to introgressive hybridization revealed by mitochondrial introgression patterns in *Ohomopterus* ground beetle assemblages. *Molecular Ecology* **16:** 4822–4836.

Nielsen R, Wakeley J. 2001. Distinguishing migration from isolation: a Markov chain Monte Carlo approach. *Genetics* **158:** 885–896.

Paetkau D, Slade R, Burden M, Estoup A. 2004. Genetic assignment methods for the direct, real-time estimation of migration rate: a simulation-based exploration of accuracy and power. *Molecular Ecology* **13:** 55–65.

Palumbi SR, Cipriano F, Hare MP. 2001. Predicting nuclear gene coalescence from mitochondrial data: the three-times rule. *Evolution* **55:** 859–868.

Piry S, Alapetite A, Cornuet JM, Paetkau D, Baudouin L, Estoup A. 2004. GENECLASS 2: a software for genetic assignment and first generation migrants detection. *Journal of Heredity* **95:** 536–539.

Posada D, Crandall KA. 1998. MODELTEST: testing the model of DNA substitution. *Bioinformatics* **14:** 817–818.

Pritchard JK, Stephens M, Donnelly P. 2000. Inference of population structure using multilocus genotype data. *Genetics* **155:** 945–959.

Rand DM, Haney RA, Fry AJ. 2004. Cytonuclear coevolution: the genomics of cooperation. *Trends in Ecology and Evolution* **19:** 645–653.

Rannala B, Mountain JL. 1997. Detecting immigration by using multilocus genotypes. *Proceedings of National Academy of Sciences of the Uinted States of America* **94:** 9197–9201.

Raymond M, Rousset F. 1995. GENEPOP (version 1.2): population genetics software for exact test and ecumenicism. *Journal of Heredity* **86:** 248–249.

Renoult JP, Geniez P, Bacquet P, Benoit L, Crochet PA. 2009. Morphology and nuclear markers reveal extensive mitochondrial introgressions in the Iberian wall lizard species complex. *Molecular Ecology* **18:** 4298–4315.

Ronquist F, Huelsenbeck JP. 2003. MrBayes 3: Bayesian phylogenetic inference under mixed models. *Bioinformatics* **19:** 1572–1574.

Rosenberg NA. 2004. DISTRUCT: a program for the graphical display of population structure. *Molecular Ecology Notes* **4:** 137–138.

Shaw KL, Lugo E. 2001. Mating asymmetry and the direction of evolution in the Hawaiian cricket genus *Laupala*. *Molecular Ecology* **10:** 751–759.

Singhal S, Moritz C. 2012. Testing hypothesis for genealogical discordance in a rainforest lizard. *Molecular Ecology* **21:** 5059–5072.

Sota T, Kubota K. 1998. Genital lock-and-key as a selective agent against hybridization. *Evolution* **52:** 1507–1531.

Stein AC, Uy JA. 2006. Plumage brightness predicts male mating success in the lekking golden-collared manakin, *Maanacus vitellinus*. *Behavioral Ecology* **17:** 41–47.

Stephens M, Smith N, Donnelly P. 2001. A new statistical method for haplotype reconstruction from population data. *American Journal of Human Genetics* **68:** 978–989.

Stoffberg S, Jacobs DS, Mackie IJ, Matthee CA. 2010. Molecular phylogenetics and historical biogeography of *Rhinolophus* bats. *Molecular Phylogenetics and Evolution* **54:** 1–9.

Strasburg J, Rieseberg LH. 2011. Interpreting the estimated timing of migration events between hybridizing species. *Molecular Ecology* **20:** 2353–2366.

Sŭsnik S, Weiss S, Odak T, Delling B, Treer T, Snoj A. 2007. Reticulate evolution: ancient introgression of the Adriatic brown trout mtDNA in softmouth trout *Salmo obtusirostris* (Teleostei: Salmonide). *Biological Journal of the Linnean Society* **90:** 139–152.

Thomas NM. 2000. Morphological and mitochondrial-DNA variation in *Rhinolophus rouxii* (Chiroptera). *Bonner Zoologische Beiträge* **49:** 1–18.

Thompson JD, Gibson TJ, Plewniak F, Jeanmougin F,

Higgins DG. 1997. The CLUSTAL_X windows interface: flexible strategies for multiple sequence alignment aided by quality analysis tools. *Nucleic Acids Research* **25:** 4876–4882.

Turmelle AS, Kunz TH, Sorenson MD. 2011. A tale of two genomes: constrating patterns of phylogeographic structure in a widely distributed bat. *Molecular Ecology* **20:** 357–375.

Van Oosterhout C, Hutchinson WF, Wills DPM, Shipley P. 2004. Micro-checker: software for identifying and correcting genotyping errors in microsatellite data. *Molecular Ecology Notes* **4:** 535–538.

Zhang D, Fengquan L, Jianmin B. 2000. Eco-environmental effects of the Qinghai-Tibet Plateau uplift during the Quaternary in China. *Environmental Geology* **39:** 1352–1358.

Zhang DX, Hewitt GM. 2003. Nuclear DNA analyses in genetic studies of populations: practice, problems and prospects. *Molecular Ecology* **12:** 563–584.

ARCHIVED DATA

Data deposited at Dryad: morphology data, microsatellite genotype data, and GenBank accession numbers for mtDNA and nuclear genes (Mao *et al*., 2013c).